Cancer Research

Modulating Bone Marrow Hematopoietic Lineage Potential to Prevent Bone Metastasis in Breast Cancer

Jessalyn M. Ubellacker[1,2], Ninib Baryawno[3,4,5], Nicolas Severe[3,4,5], Molly J. DeCristo[1,2], Jaclyn Sceneay[1,2], John N. Hutchinson[6], Marie-Therese Haider[7], Catherine S. Rhee[3,4,5], Yuanbo Qin[1,2], Walter M. Gregory[8], Ana C. Garrido-Castro[9], Ingunn Holen[7], Janet E. Brown[7], Robert E. Coleman[7], David T. Scadden[3,4,5,10], and Sandra S. McAllister[1,2,5,10]

Abstract

The presence of disseminated tumor cells in breast cancer patient bone marrow aspirates predicts decreased recurrence-free survival. Although it is appreciated that physiologic, pathologic, and therapeutic conditions impact hematopoiesis, it remains unclear whether targeting hematopoiesis presents opportunities for limiting bone metastasis. Using preclinical breast cancer models, we discovered that marrow from mice treated with the bisphosphonate zoledronic acid (ZA) are metastasis-suppressive. Specifically, ZA modulated hematopoietic myeloid/osteoclast progenitor cell (M/OCP) lineage potential to activate metastasis-suppressive activity. Granulocyte-colony stimulating factor (G-CSF) promoted ZA resistance by redirecting M/OCP differentiation. We identified M/OCP and bone marrow transcriptional programs associated with metastasis suppression and ZA resistance. Analysis of patient blood samples taken at randomization revealed that women with high-plasma G-CSF experienced significantly worse outcome with adjuvant ZA than those with lower G-CSF levels. Our findings support discovery of therapeutic strategies to direct M/OCP lineage potential and biomarkers that stratify responses in patients at risk of recurrence.

Significance: Bone marrow myeloid/osteoclast progenitor cell lineage potential has a profound impact on breast cancer bone metastasis and can be modulated by G-CSF and bone-targeting agents. *Cancer Res; 78(18); 5300–14. ©2018 AACR.*

Introduction

The majority of patients with breast cancer have no evidence of metastatic disease at the time of diagnosis, yet approximately 30% of patients experience recurrent breast cancer in the form of metastasis, of which the most prominent site is bone (1). Moreover, bone is the most frequent site of *de novo* metastasis for all breast cancer molecular subtypes (2). At present, little is known about what promotes tumor cell survival and outgrowth into incurable disease in the bone (1, 3). Disseminated tumor cells (DTC) are frequently detected in bone marrow aspirates of patients with breast cancer, regardless of breast cancer subtype and even in those who have early-stage disease, and are predictive of decreased recurrence-free survival (4). These and other such findings support the idea that DTCs find a hospitable niche in the bone marrow (4–6).

Bone metastatic niches in which DTCs reside have been defined as microdomains within the bone that support tumor cell seeding and outgrowth and are predominantly comprised of hematopoietic cells, mesenchymal stromal cells, osteoblasts, osteoclasts, and/or vascular cells (5, 6). Paracrine interactions between DTCs and these various stromal cells disrupt bone homeostasis, which is normally tightly controlled, to fuel metastatic progression. For example, it is well established that DTCs secrete a variety of cytokines that promote osteoclast activity, which in turn, causes release of a variety of tumor-promoting growth factors from the bone, thus propagating a vicious cycle of tumor outgrowth and osteolytic bone breakdown (6).

Although results from studies that focused on mesenchymal stromal cells, osteoblasts, osteoclasts, and vascular cell activity have yielded significant insights into cellular and molecular processes that influence DTC outgrowth and dormancy in the bone (5, 6), surprisingly little is known about whether or how hematopoietic cells in the marrow compartment impact bone

[1]Hematology Division, Brigham & Women's Hospital, Boston, Massachusetts. [2]Department of Medicine, Harvard Medical School, Boston, Massachusetts. [3]Department of Stem Cell and Regenerative Biology, Harvard University, Cambridge, Massachusetts. [4]Center for Regenerative Medicine and the Cancer Center, Massachusetts General Hospital, Boston, Massachusetts. [5]Harvard Stem Cell Institute, Cambridge, Massachusetts. [6]Department of Biostatistics, Harvard T.H. Chan, School of Public Health, Boston, Massachusetts. [7]Academic Unit of Clinical Oncology, Department of Oncology & Metabolism, Weston Park Hospital, University of Sheffield, Sheffield, United Kingdom. [8]Clinical Trials Research Unit, University of Leeds, Leeds, United Kingdom. [9]Department of Medical Oncology, Dana-Farber Cancer Institute, Boston, Massachusetts. [10]Broad Institute of Harvard and MIT, Cambridge, Massachusetts.

Note: Supplementary data for this article are available at Cancer Research Online (http://cancerres.aacrjournals.org/).

Corresponding Author: Sandra S. McAllister, Harvard Medical School, Brigham & Women's Hospital, 4 Blackfan Circle, HIM 742, Boston, MA 02215. Phone: 617-525-4929; Fax: 617-355-9093; E-mail: smcallister1@bwh.harvard.edu

doi: 10.1158/0008-5472.CAN-18-0548

metastases. Clinical studies indicate that the presence of DTCs in patient with breast cancer bone marrow correlates with metastatic relapse and poor outcome (7). In the preclinical setting, it is becoming increasingly apparent that various physiologic and pathologic processes as well as certain drugs and chemotherapies alter hematopoietic cells in the marrow in ways that impact cancer progression (7–10); however, it is not yet clear how DTCs are impacted when they first encounter such hematopoietic cells in the marrow.

Hematopoiesis relies on precise regulation of quiescence, proliferation, and differentiation of hematopoietic progenitor cells within specialized niches (11, 12). For example, within the osteoblastic niche, mature osteoclasts influence hematopoiesis by releasing bone-matrix proteins essential for hematopoietic cell maintenance (13, 14). It is reasonable therefore to hypothesize that modulating osteoclast activity would have an impact on hematopoiesis in ways that affect DTC behavior.

We previously established that bisphosphonate treatment, which is a widely used osteoclast inhibitor therapy for effective treatment of osteolytic diseases, induces subclinical changes in the composition of bone marrow hematopoietic progenitor populations (15). We reported that bone marrow cells isolated from zoledronic acid (ZA)-treated animals suppress mammary carcinoma formation in the absence of a direct effect of ZA on tumor cells, indicating that the bone marrow harbors the majority of ZA's tumor-suppressive capacity (15). However, whether such modulation of the marrow affects breast cancer bone metastasis independently of the effects on mature osteoclasts in the endosteal niche and whether a specific subpopulation of hematopoietic cells has metastasis-suppressive capacity remained undetermined. A better understanding of the bone marrow microenvironment and processes that influence tumor cell maintenance and growth in the bone should present opportunities for targeting hematopoietic cell populations as part of anticancer therapy.

Materials and Methods

Cell lines

MDA-MB-231 B1 cells (gift from Dr. Gabri van der Pluijm, Leiden University Medical Centre, Leiden, South Holland, Netherlands), a clonal bone-tropic human breast cancer cell line expressing luciferase, was maintained under selection in 1 mg/mL gentamicin, (G418, Life Technologies, 15750060) in DMEM with 10% FBS. MDA-MB-231 B2 bone-tropic human breast cancer cells (gift from Dr. Penelope Ottewell, Department of Onocology and Metabolism, University of Sheffield, Sheffield, United Kingdom) were transfected with luciferase and maintained in 10% FBS in DMEM. Cells were not used beyond passage five post-thawing. All cells tested negative for *Mycoplasma* (Lonza Kit: LT07-118) every 6 months (last test: June 2017) and were validated using short tandem repeat (STR) profiling (Molecular Diagnostics Laboratory at Dana-Farber Cancer Institute, Boston, MA).

Mice

Six to 7-week-old female CrTac:NCr-*Foxn1*^{nu} (nude) female mice were purchased from Taconic Laboratories. C57BL/6J female mice were purchased from The Jackson Laboratory. All animal procedures were performed in accordance with the ethics and regulations of Brigham & Women's Hospital Institutional Animal Care and Use Committee (protocol approval 2017N000056), Boston Children's Hospital Institutional Animal Care and Use Committee (protocol approval 12-11-2308R), and Massachusetts General Hospital (protocol approval 2017N000023).

Drug administration

ZA [1-hydroxy-2-(1H-imidazole-1-yl)ethylidene-bisphosphonic acid] (Novartis Pharmaceuticals) was dissolved in 1× Hank balanced buffer solution (Gibco) and stored at 4°C until use. ZA was administered to mice at a dose of 100 μg/kg (i.p.). Recombinant human granulocyte-colony stimulating factor (G-CSF; carrier-free, BioLegend #578604) was administered to nude mice each day for 3 days at a dose of 50 μg/kg (i.p.) beginning one day after administration of ZA, and C57BL/6 mice each day for 3 days at a dose of 50 μg/kg (i.p.) beginning 2 days after administration of ZA. For G-CSF depletion experiments, nude mice were treated with 100 μg/kg (i.p.) G-CSF antibody (R&D Systems, MAB414100) or the 100 μg/kg (i.p.) isotype control IgG (R&D Systems, MAB005) 6 hours prior to intracardiac injection of tumor cells.

Blood and plasma

At experimental endpoints, blood was collected by intracardiac puncture with a 27-gauge needle into ethylenediaminetetraacetic acid (EDTA) Microtainer tubes (BD Pharmingen). Complete blood counts were obtained using a HEMAVET hematology analyzer (Drew Scientific). Plasma was prepared by centrifugation of whole blood at 1.5 g × 1,000 for 8 minutes at 4°C.

Experimental bone metastasis

Mice were anesthetized with isoflurane, and 1×10^5 luciferase-tagged bone-tropic cell lines (B1, B2, B1-G, B2-shG) were suspended in 100 μL of PBS and injected into the left cardiac ventricle. Tumor growth was monitored by bioluminescence imaging, and by Vybrant CM-Dil cell-labeling solution by florescence imaging (Life Technologies, V22888). For intratibial injections, mice were anesthetized with isoflurane and 5×10^4 cells in 10 μL of PBS were injected directly into both tibiae. Tumor growth was monitored by bioluminescence imaging. In indicated experiments, mice were treated with 100 μg/kg of ZA or equivalent volume of vehicle control 72 hours prior to injection of tumor cells.

Bone marrow cell preparations

Femora and tibiae were dissected free into 2% FBS in PBS and centrifuged at 6.0–7.0 g ×1,000 for 4 minutes at 4°C to collect whole bone marrow cells (BMC; WBM). Cells were then incubated with red blood cell (RBC) lysis solution (BioLegend, 420301) for 5 minutes on ice, washed once with 2% FBS in PBS, resuspended in 0.5 mL of sterile BMC buffer, and passed through a 5-mL polystyrene round-bottom tube with a cell-strainer cap (Corning, 352235).

Flow cytometry and FACS

BMCs were prepared for flow cytometry by suspension in sterile PBS containing 2% FBS. Cells were labeled with appropriate antibodies for 30 minutes at 4°C. Gating was used to exclude debris, cell clumps, and dead cells (using 7-aminoactinomycin D; 7-AAD Viability Staining Solution (BioLegend, 420404). Myeloid/osteoclast progenitor cell (M/OCP) populations were defined as Lineage$^-$ CD115$^+$. Antibody panel includes Pacific Blue anti-mouse Lineage Cocktail (BioLegend, 133310: CD3$^-$, Ly-6G/Ly6-C$^-$, Cd11b$^-$, CD45R$^-$, TER119$^-$) and Alexa Fluor 488

anti-mouse CD115 (CSF-1R; BioLegend, 135511). Cells were acquired on a FACSCanto II or a FACSAria IIu/FACSDiva (BD Biosciences). At the endpoint of the osteoclast differentiation assays, macrophages were defined as $MHCII^+/F4/80^+/Cd11b^+$ (MHCII: APC-Cy7 (BioLegend 107627), F4/80: PE-Cy-7 (BioLegend 123113), Cd11b:Alexa Fluor-488 (BioLegend 101205) and dendritic cells were defined as $MHCII^+/Cd11b^+/Cd11c^+$ [MHCII: APC-Cy7 (BioLegend 107627), Cd11c: PE (BioLegend 117307), Cd11b:Alexa Fluor-488 (BioLegend 101205)]. Analyses were performed using FlowJo software (FlowJo, LLC). CountBright Absolute Counting Beads (Life Technologies, C36950) were used to quantify absolute cell numbers. For cell sorting of the M/OCP populations and for isolation of Lin^- and Lin^+ populations, the Murine Direct Lineage Cell Depletion Kit (Miltenyi Biotec Inc., 130-110-470) was used to enrich for Lin^- populations, which was confirmed by flow cytometry for the markers in the lineage cocktail.

Bone marrow tumor support functional assay

Donor mice were treated via intraperitoneal injection with vehicle (1× HBBS) or ZA (100 μg/kg) and sacrificed 3 days (nude mice) or 5 days (C57BL/6 mice) following treatment. BMCs were harvested as described above. For WBM assays, 7.5×10^5 donor BMCs were mixed with 2.5×10^5 of the appropriate tumor cells in 100 μL DMEM with 10% basement membrane matrix, Corning Matrigel Growth Factor Reduced (low growth; Westnet Inc., 354230) immediately prior to injection. To test the tumor support function of various FACS-isolated marrow subpopulations, 2.5×10^5 tumor cells were mixed with either 2.5×10^5 Lin^- BMCs, 7.5×10^5 Lin^+ BMCs, or 1×10^5 M/OCPs. Admixtures were injected subcutaneously into host nude mice. During the 14-day time courses, no graft versus host disease was observed for nude mice receiving C57BL/6 donor marrow. Each donor BMC sample was distributed into a minimum of 3 host nude mice. Tumor growth was monitored by bioluminescent imaging.

Osteoclast differentiation assay

Bone marrow cells were prepared as previously described, and 1,000 WBM cells or 250 M/OCP cells were plated in 24-well plates with 15% FBS in αMEM with 10 ng/mL of recombinant M-CSF (R&D Systems, 416ML010). After 3 days, recombinant RANKL (5 ng/mL R&D Systems, 462TEC010CF) or vehicle control were added to the assay. At the 5-day endpoint, Tartrate Resistant Acid Phosphatase, Leukocyte (TRAP) Kit (Sigma Aldrich, 387A) was used and TRAP-positive osteoclasts were counted and flow cytometry was performed to quantify the numbers of macrophages and dendritic cells in the resultant cultures. To test phagocytic function of the resulting cultures, tumor cells were stained with Vibrant CM-Dil (Life Technologies) at a concentration of 5 μL CM-Dil solution per 1 million cells/mL for 5 minutes at 37°C. Cells were washed twice with PBS, and then 1,000 tumor cells were added into the wells at the endpoint of the osteoclast differentiation assay. After two hours, wells were washed with PBS and prepared for flow cytometry. Cells within the macrophage gate that were $CM\text{-}Dil^+$ were reported as a percentage of the total macrophage population.

Patient plasma samples

Breast cancer patient plasma samples ($n = 392$) were obtained from the AZURE clinical trial sample database (ISRCTN79831382, University of Sheffield, Sheffield, United Kingdom; ref. 16). The AZURE study was performed in accordance with the Declaration of Helsinki, and was performed after approval by an institutional review board (West Midlands Research Ethics Committee). Patients were randomized to either standard adjuvant therapy alone (control, Ctl) or with ZA (Novartis Pharmaceuticals) and written informed consent was received from all patients prior to inclusion in the study. To reduce possible imbalances in tumor and treatment characteristics, a minimization process was used that took into account the number of involved axillary lymph nodes, clinical tumor stage, estrogen receptor status, type and timing of systemic therapy, menopausal status, statin use, and treating center. Eligible patients were randomized to receive (neo) adjuvant chemotherapy and/or endocrine therapy ± ZA 4 mg i.v. every 3–4 weeks for 6 doses, then 3 monthly ×8 and 6 monthly ×5 to complete 5 years of treatment. Secondary prophylaxis with G-CSF to prevent neutropenic sepsis or treatment delays due to neutropenia was allowed but primary G-CSF prophylaxis was not used. Both the use of adjuvant systemic treatments and locoregional radiotherapy were given in accordance with standard protocols at each participating institution. The date of recurrence was defined as the date on which relapse was first suspected. Subjects were followed up on an annual basis after completion of the 5-year treatment phase (ZA or Ctl) for both disease and relevant safety endpoints (16). Patient samples to be used in this study were selected on the basis of: (i) menopausal status [postmenopausal women ($n = 164$); non-postmenopausal women ($n = 226$); unknown menopausal status ($n = 2$)], (ii) whether or not the patient had recurrence of breast cancer (disease-free or recurrence in bone only or bone as well as other distant sites), and (iii) whether or not the patient received adjuvant ZA treatment. These three parameters were used to power the sample size estimation using the reported HR of 0.81, and a standardized effect size of 0.80 (16). Plasma G-CSF levels were analyzed by ELISA.

Statistical analysis

All experiments were performed with three independent replications, unless otherwise indicated. Sample size for *in vivo* experiment was based on outcomes from pilot experiments and was calculated at a statistical significance level of 0.05, and powered at 0.80. All data were analyzed with the use of GraphPad Prism Software (Version 7). Data are expressed as mean ± SEM with n denoting the number of independent data points (i.e., mice, cell wells, etc.). Statistics were determined using the unpaired, two-tailed Student t test unless otherwise indicated. Results were considered statistically significant if $P < 0.05$ (*), $P < 0.01$ (**), and $P < 0.001$ (***).

ELISAs and cytokine array

Plasma was obtained from the mice as previously described, and ELISA assays were performed according to manufacturer's instructions: Murine G-CSF ELISA Kit (R&D Systems, MCS00); Murine RANKL ELISA Kit (Innovative Research, IRKTAH5466); Murine NTX ELISA (Biotang Inc., 50154363). For the human cytokine array, 1×10^5 cells of B1 or B2 were plated and conditioned media from 5 different wells was obtained 24 hours after plating, was pooled and then assessed using Human Cytokine Array, Panel A per manufacturer's instructions (R&D Systems,

ARY005). For the patient plasma samples, 100 μL of sample was used and ELISA assays were performed according to manufacturer's instructions (Human G-CSF QKIT HS ELISA; R&D Systems, HSTCS0). Plates were analyzed using Softmax Pro7 Software (Molecular Devices).

Data and software availability

RNA-Sequencing data will be available using the Gene Expression Omnibus (GEO; GSE108250) database.

Results

Identification of therapeutically induced tumor-inhibitory hematopoietic bone marrow cells

We and others have reported that primary cancers, physiologic aging, and drug treatments all affect bone marrow hematopoietic cells in ways that influence disease progression (8–10, 15, 17). To understand whether therapeutic modulation of the bone marrow microenvironment would provide an effective approach for treating breast cancer bone metastasis, we used the nitrogen-containing bisphosphonate, ZA in both immunocompromised and immunocompetent preclinical models of breast cancer.

We treated tumor-free cohorts of C57BL/6 and nude mice with a single dose of either ZA or vehicle control and harvested their bone marrow 5 days (C57BL/6 mice) or 3 days (nude mice) following treatment. These are time points at which osteoclast activity is inhibited by ZA (15). We then used our well-established hematopoietic cell functional assay (15–18) to test the bone marrow for effects on growth of a bone-metastatic human breast tumor cell line, MDA-MB-231-B1 (B1), (Fig. 1A). This assay is designed to test any effects on tumor growth that are exclusively mediated by bone marrow hematopoietic cells and is based on the notion that the outgrowth of DTCs would be affected by any ZA-induced changes to hematopoietic cells. Importantly, mature osteoclasts are of hematopoietic origin but localize to the endosteal niche upon maturation (19). TRAP staining of the bone marrow plugs confirmed that osteoclasts were absent from the bone marrow samples used in these experiments (Supplementary Fig. S1A).

WBM from both strains of Ctl-treated donor mice had no significant effect on subcutaneous B1 tumor growth when compared with B1 tumor cells injected alone—in these cohorts, tumors formed with approximately 80% incidence in both strains of mice (Fig. 1B; Supplementary Fig. S1B). However, WBM from both strains of ZA-treated mice significantly reduced B1 tumor incidence to <30% (Fig. 1B; Supplementary Fig. S1B), indicating that tumor suppression occurred independently of a functional adaptive immune system.

To begin to understand whether tumor-suppressive function is enriched in a particular subpopulation of hematopoietic cells, we sorted the marrow from Ctl or ZA-treated mice into lineage-negative (Lin^-) progenitor populations and mature lineage-positive (Lin^+) populations and assessed B1 tumor growth using the bone marrow functional assay. As before, WBM from the ZA-treated mice suppressed B1 tumor formation; tumor incidence was only 50% of that from the respective Ctl cohort (Fig. 1C). The Lin^+ subpopulation from ZA-treated mice had no effect on tumor incidence, which was equivalent to that of the respective Ctl subpopulation (Fig. 1C). In striking contrast, Lin^- cells from ZA-treated donors significantly reduced B1 tumor incidence to only 14.3% relative to Lin^- cells from the Ctl mice (Fig. 1C).

Osteoclasts differentiate from Lin^- myeloid-committed cells in the marrow (19–21); therefore, we wondered whether ZA imparted its tumor-suppressive effect via osteoclast precursor cells. There is currently no clear consensus on the cell-surface markers that delineate osteoclast precursors (21). However, given our previous report that ZA, in addition to inhibiting osteoclast activity, significantly expands numbers of bone marrow common myeloid progenitor populations (15), we reasoned that an effort to capture functional activity should include multipotent progenitors of the myeloid/osteoclast lineage. We therefore utilized the markers $CD3^-B220^-Ly6G^-Ly6C^-CD11b^-Ter119^-CD115^+$ to define a population we termed "myeloid/osteoclast progenitors" (M/OCP; Supplementary Fig. S1C). We confirmed that this sorted population from Ctl-treated donors gives rise to macrophages, dendritic cells, and osteoclasts in a standard *in vitro* differentiation assay (Supplementary Fig. S1D and S1E; ref. 20).

We treated tumor-free C57BL/6 mice with a single dose of ZA and quantified the numbers of $CD3^-B220^-Ly6G^-Ly6C^-CD11b^-Ter119^-CD115^+$ M/OCPs in the marrow over an experimental time course of 15 days. ZA treatment significantly increased the number of bone marrow M/OCPs in a time-dependent manner (Fig. 1D).

We then investigated M/OCP tumor-suppressive function by sorting $CD3^-B220^-Ly6G^-Ly6C^-CD11b^-Ter119^-CD115^+$ M/OCPs, as well as the M/OCP-depleted population, from the marrow of Ctl or ZA-treated cohorts and subjecting them to the bone marrow functional assay. As a control, we confirmed that WBM from the ZA-treated cohort significantly suppressed tumor growth as expected (Fig. 1E; Supplementary Fig. S1F). M/OCPs isolated 5 days after ZA treatment significantly inhibited tumor incidence and mass relative to the same number of M/OCPs from the Ctl-treated cohort (Fig. 1E; Supplementary Fig. S1F). In contrast, the M/OCP-depleted marrows from Ctl and ZA-treated mice were not significantly different in their tumor-modulating capacity (Fig. 1E).

The results from the *in vivo* BMC functional assays suggested that M/OCPs from ZA-treated mice are qualitatively different than their control counterparts. Hence, we performed RNA sequencing on M/OCPs from Ctl and ZA-treated cohorts. Computational analyses revealed a list of significantly differentially expressed genes (DEG; GEO, GSE108250; Supplementary Table S1). Functionally enriched gene ontology (GO) terms and gene set enrichment analyses (GSEA) among the DEGs revealed biological and cellular processes that were enriched in the ZA-treated M/OCPs. Of these, "organic cyclic compound metabolic process," "cellular aromatic compound metabolic process," "oxidative phosphorylation," "phagosome," "lysosome organization," and "lipid transport" pathways (Fig. 1F; Supplementary Table S2A and S2B) were particularly interesting, as these processes are important for monocyte differentiation and macrophage function (22, 23).

Collectively, these results established that M/OCP transcriptional programs are altered in the marrow and correlate with tumor-suppressive function in response to the bone-targeting agent, ZA, independently of a functional adaptive immune system. Moreover, these results are in agreement with preclinical findings that ZA reduces the risk of breast cancer recurrence independently of its direct action on osteoclast apoptosis (24)

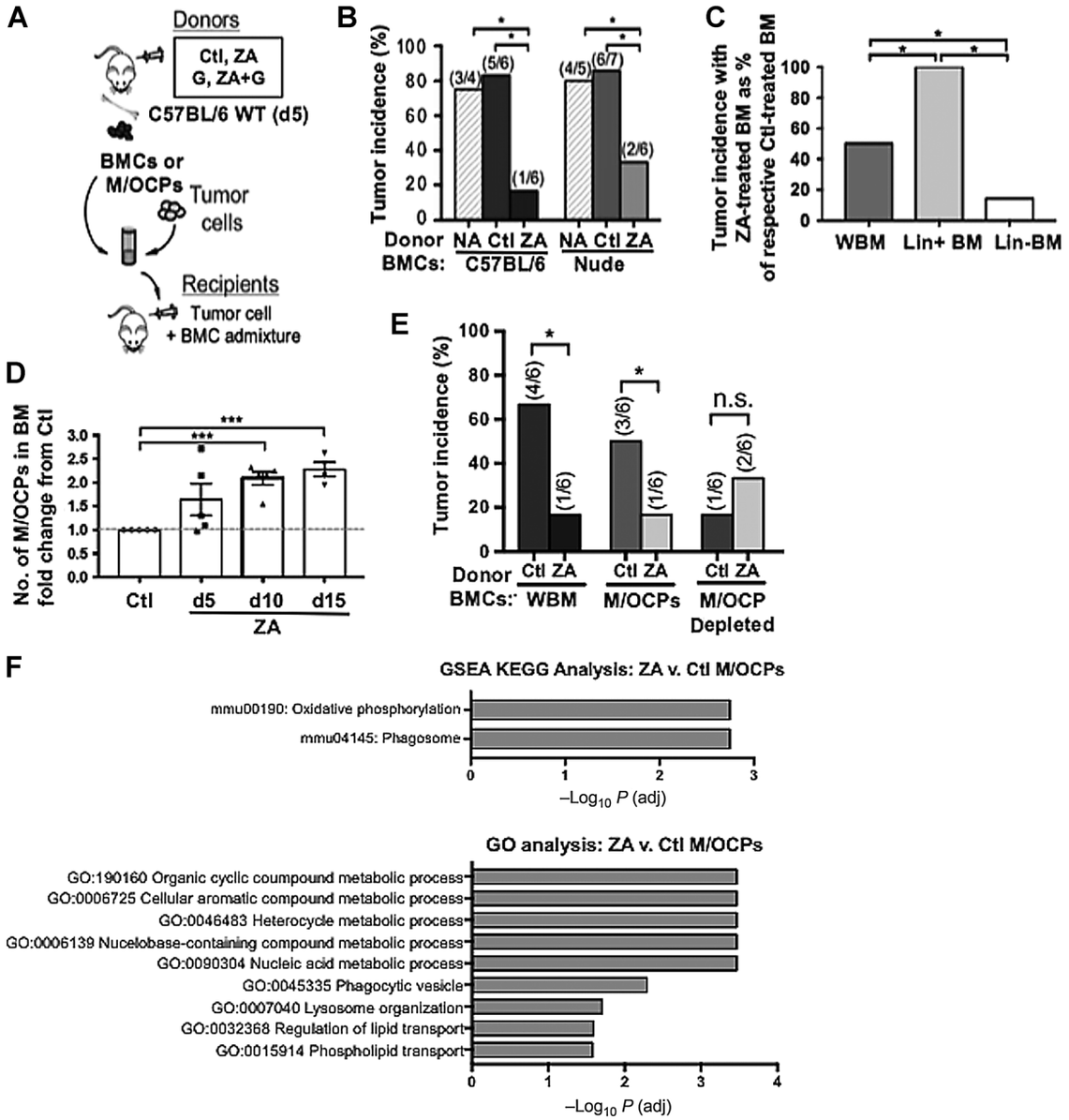

Figure 1.

Identification of therapeutically induced tumor-inhibitory hematopoietic bone marrow cells. **A,** Experimental scheme for assay to test BMC tumor support function. WBM or various FACS-isolated bone marrow populations were harvested from ZA- or vehicle-treated control (Ctl) donor mice at either 5 days (C57BL/6) or 3 days (nude) and mixed with tumor cells immediately prior to injection into recipient mice and tumor incidence and growth kinetics measured over time. **B,** Incidence (%) of subcutaneous tumor formation in nude recipient mice at experimental endpoint (d14) resulting from 2.5×10^5 MDA-MB-231-B1 (B1) cells admixed with Matrigel (NA, no donor BMCs included) or 7.5×10^5 WBM cells from Ctl or ZA-treated nude and C57BL/6 donors ($n = 4$–7 injections per cohort; statistics representative of two biological replicates). **C,** Incidence (%) of subcutaneous tumor formation in nude recipient mice at experimental endpoint (d14) resulting from 2.5×10^5 MDA-MB-231-B1 (B1) cells admixed with 7.5×10^5 WBMs, 7.5×10^5 Lin^+ BMCs, or 2.5×10^5 Lin- BMCs from Ctl- or ZA-treated nude donors. Data for each ZA-treated cohort are represented relative to its respective Ctl-treated cohort; ($n = 20$–24 injections per cohort). Lin^- populations were sorted by gating on $CD3^-$ Ly-6G/Ly6-C^- $Cd11b^-$ $CD45R^-$, and $TER119^-$ and all of the remaining BMCs were used as the Lin^+ populations. **D,** Number of M/OCPs (Lin^-CD115^+) in the bone marrow of C57BL/6 mice at indicated time points after ZA treatment ($n = 4$–5 mice per cohort, representative of three biological replications). **E,** Incidence (%) of tumor formation in nude recipient mice at experimental endpoint (d14) resulting from 2.5×10^5 B1 cells admixed with 7.5×10^5 WBM cells, 10^5 sorted M/OCPs, or 6.5×10^5 M/OCP-depleted BMCs from Ctl- or ZA-treated C57BL/6 donors ($n = 6$ injections per cohort; statistics representative of two biological replications). Controls from different cohorts were not compared due to the fact that different numbers of BMCs were admixed with tumor cells in each case. **F,** GSEA analysis [clusterProfiler tool using Kyoto Encyclopedia of Genes and Genomes (KEGG) gene sets] and gprofileR (GO) analysis of the differentially expressed genes in M/OCPs isolated from ZA-treated mice as compared with M/OCPs isolated from Ctl-treated mice. Significance was determined as described in Materials and Methods: RNA-sequencing. Error bars, mean ± SEM; two-tailed *t* tests (unpaired) were used to determine statistical significance (*, $P < 0.05$; ***, $P < 0.001$). n.s., nonsignificant.

and that bone tumor burden can be modulated in an osteoclast-independent manner (25).

ZA skews lineage potential of myeloid/osteoclast progenitor cells toward macrophages

Our RNAseq analyses suggested that M/OCPs are enriched for transcriptional programs consistent with those of the monocyte/macrophage lineage in response to ZA. Although it is well known that ZA inhibits mature osteoclasts, whether ZA affects myeloid/osteoclast lineage bias is not understood; therefore, we tested the lineage potential of bone marrow samples from control and ZA-treated mice using *in vitro* differentiation assays (20; Fig. 2A). In these assays, macrophage-colony stimulating factor (M-CSF; CSF1) is necessary for sustaining M/OCP populations (26) and in the absence of receptor activator of nuclear factor kappa-B ligand (RANKL), these progenitors normally differentiate into macrophages and dendritic cells (DC) whereas in the presence of RANKL, they differentiate into osteoclasts (27).

Interestingly, when WBM samples from ZA- and Ctl-treated mice were subjected to M-CSF and RANKL *in vitro*, the marrow cells from ZA-treated donors gave rise to significantly fewer numbers of osteoclasts as compared with those of Ctl-treated donors (Fig. 2B), despite having more M/OCPs (Fig. 1D). Instead, the resulting cultures from the ZA-treated cohort had significantly increased numbers of macrophages ($Cd11b^+$/$F4/80^+$/$MHCII^+$) and DCs ($Cd11b^+$/$MHCII^+$/$Cd11c^+$) as compared with those of the Ctl-treated cohort (Fig. 2C; Supplementary Fig. S2A and S2B). In fact, these numbers of macrophages and DCs were comparable with those of bone marrow samples treated only with M-CSF (Fig. 2C).

We next tested the lineage potential of M/OCPs isolated from ZA-treated animals. Thus, we sorted M/OCP populations from the marrow of mice treated with Ctl or ZA and subjected them to the differentiation assay. In the presence of RANKL, M/OCPs from ZA-treated mice gave rise to significantly more macrophages than those of controls and these numbers were comparable to those from cultures that had not been treated with RANKL (Fig. 2D). Although DCs were detected in the resulting cultures, there were no significant differences in their numbers between ZA and Ctl treated mice (Fig. 2D; Supplementary Fig. S2B).

Collectively, these findings indicated that ZA inherently changes the lineage potential of M/OCPs by skewing their differentiation potential toward macrophages, even in the presence of RANKL. Moreover, the marrow of ZA-treated cohorts harbor significantly more of these differently poised M/OCPs than that of the control counterparts.

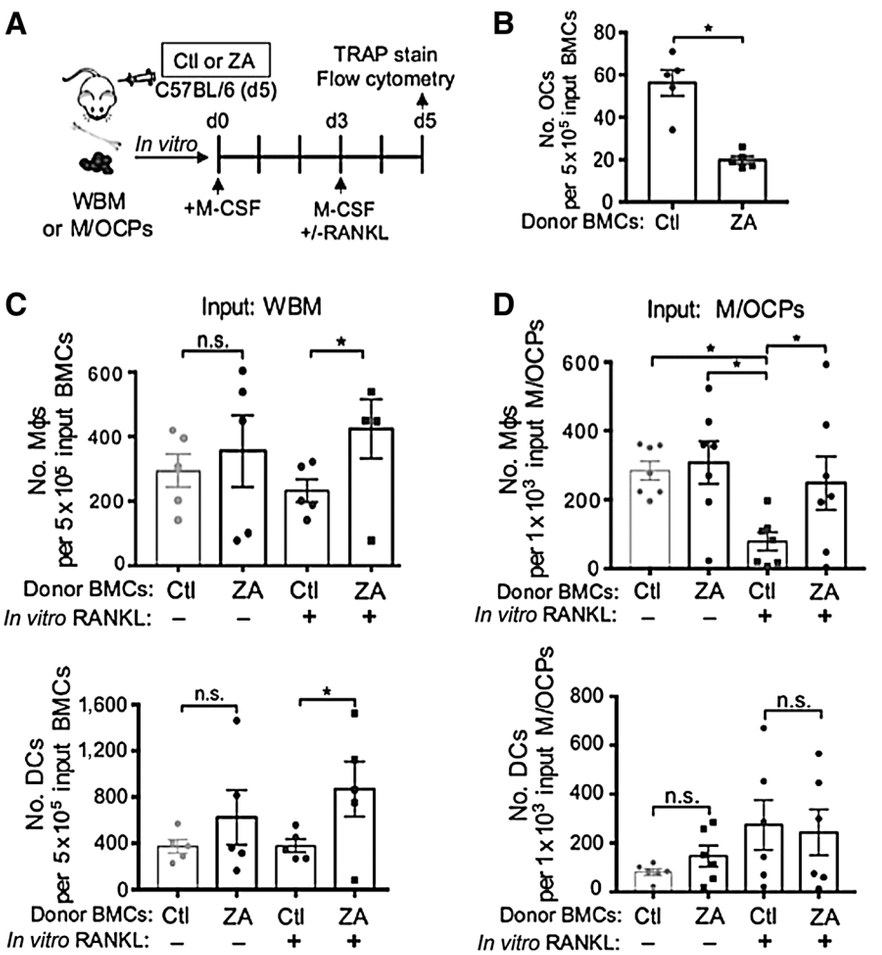

Figure 2.

ZA skews lineage potential of myeloid/osteoclast progenitor cells toward macrophages. **A,** Experimental scheme for *in vitro* osteoclast differentiation assay with WBM or M/OCPs from Ctl- or ZA-treated C57BL/6 donors. **B,** Quantification of osteoclasts (OC) ($TRAP^+$, multinucleated cells) at endpoint of *in vitro* osteoclast differentiation assay (d5) with WBM from Ctl- or ZA-treated C57BL/6 donors ($n = 5$ donor samples/cohort; representative of three biological replicates). **C** and **D,** Flow cytometric quantification of macrophages (Mϕs; $Cd11b^+$/$F4/80^+$/$MHCII^+$) and DCs ($Cd11b^+$/$MHCII^+$/$Cd11c^+$) from sorted WBM populations (**C**; $n = 5$ donor samples/cohort; representative of three biological replicates) or M/OCPs (**D**; $n = 6$–7 donor samples/cohort; representative of three biological replicates) from Ctl- or ZA-treated C57BL/6 donors at endpoint (d5) of osteoclast differentiation assay. Error bars, mean ± SEM; two-tailed *t* tests (unpaired) were used to determine statistical significance (*, $P < 0.05$). n.s., nonsignificant.

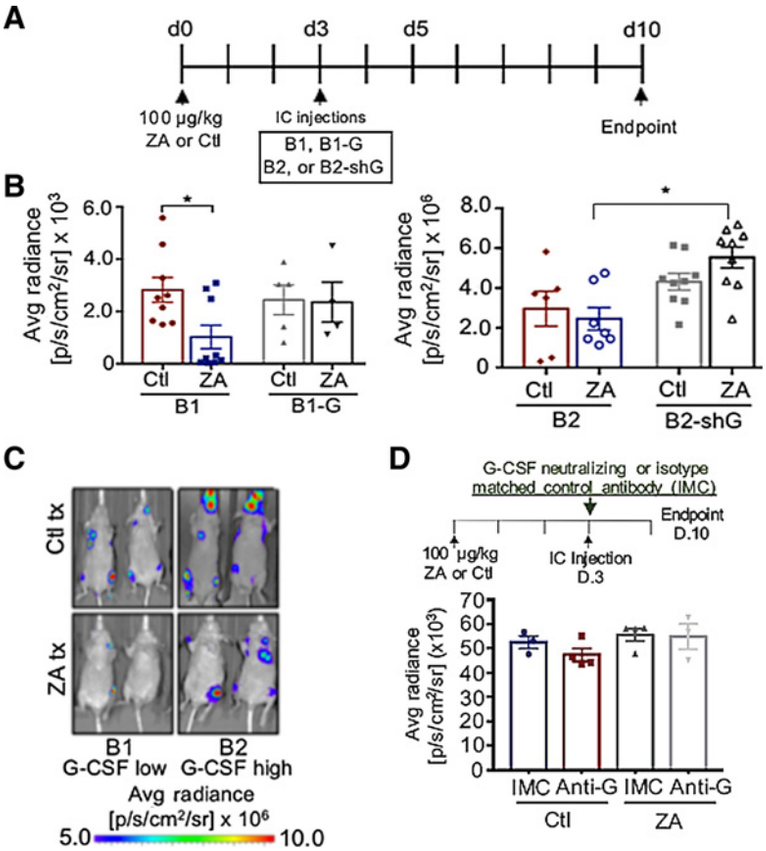

Figure 3.
ZA inhibits breast cancer metastasis in a manner that is counteracted by G-CSF. **A,** Experimental scheme for intracardiac (IC) injections of indicated breast tumor cells into Ctl or ZA pretreated nude mice. **B,** Total tumor burden at experimental endpoint as quantified by bioluminescence imaging (n = 4–9/cohort); representative of three biological replicates. **C,** Representative bioluminescence images from indicated cohorts in **B** at experimental endpoint. **D,** Experimental scheme for intracardiac injections of B2 cell line following pretreatment with Ctl or ZA and a G-CSF neutralizing antibody or isotype-matched control antibody (IMC; top). Graph represents total tumor burden at experimental endpoint (d10) as quantified by bioluminescence imaging of the luciferase$^+$ B2 cell line. All mice had signal present (d10; n = 4–5/cohort). Error bars, mean ± SEM; two-tailed t tests (unpaired) were used to determine statistical significance (*, $P < 0.05$).

ZA inhibits breast cancer metastasis in a manner that is counteracted by G-CSF

The ability to therapeutically generate tumor-suppressive bone marrow has important implications for bone metastasis; therefore, we tested whether pretreating nude mice with ZA three days prior to intracardiac injection of breast tumor cells would affect subsequent bone metastasis (Fig. 3A). We used two derivative bone-tropic subpopulations, B1 (28) and B2 (29), of the parental MDA-MB-231 breast cancer cell line.

Interestingly, while B1 bone metastatic burden was significantly lower following ZA pretreatment (63.7% lower than the control cohort, $P < 0.05$), B2 metastatic burden was unaffected (Fig. 3B and C; Supplementary Fig. S3A). Likewise, ZA pretreatment decreased outgrowth of B1, but not B2, bone tumors when cells were directly injected into the tibia (Supplementary Fig. S3B). Moreover, WBM from ZA-treated mice did not suppress B2-derived tumor growth in the bone marrow functional assay (Supplementary Fig. S3C), indicating that the B2 cell line is resistant to the tumor-suppressive effect of ZA-treated bone marrow.

Comparative cytokine analysis revealed that the ZA-resistant B2 cell line expressed higher levels of G-CSF, GM-CSF, CXCL1, and IL18 than the ZA-responsive B1 cell line (Supplementary Fig. S3D). Various tumor-derived factors have been previously shown to induce osteoclastogenesis and osteoclast activity, including cell surface ligand Jagged1 and secreted factors RANKL, G-CSF, GM-CSF, MIP-1α, PTHrP, IL8, IL6, ICAM1 (30, 31). In particular, elevated plasma levels of G-CSF have been correlated with poor prognosis for patients with triple-negative breast cancer (32) and enhanced osteoclast activity has been reported in mice with elevated G-CSF levels (33–35). Although it is well established that G-CSF leads to increased numbers of myeloid cells in the bone marrow (35), whether G-CSF directly affects osteoclastogenesis or response to ZA is not well understood.

To assess whether G-CSF plays a role in resistance to ZA treatment that we had observed, we overexpressed G-CSF in the B1 cell line, which has endogenously low G-CSF expression, to generate a G-CSF–high cell line (B1-G) (Supplementary Fig. S3E). Unlike the B1 bone metastases that were significantly reduced following ZA pretreatment (~3-fold reduction; $P < 0.05$), the B1-G metastatic burden was no different from that of the control cohort and significantly higher than that of B1 cells treated with ZA (Fig. 3B and C). ZA also failed to suppress B1 metastases when G-CSF was administered systemically (Supplementary Fig. S3F), even though the systemic efficacy of G-CSF was confirmed by an expected increase in peripheral neutrophil counts (Supplementary Fig. S3G). Of note, neutrophil numbers in the bone marrow of B1 tumor-bearing mice was unchanged after ZA, G-CSF, or ZA+G-CSF administration (Supplementary Fig. S3H) and G-CSF did not alter osteoclast activity relative to Ctl treatment, as measured by plasma NTX (Supplementary Fig. S3I).

To determine whether G-CSF suppression is sufficient to confer ZA response, we used two different shRNA constructs to suppress G-CSF in the B2 cell line, which has endogenously

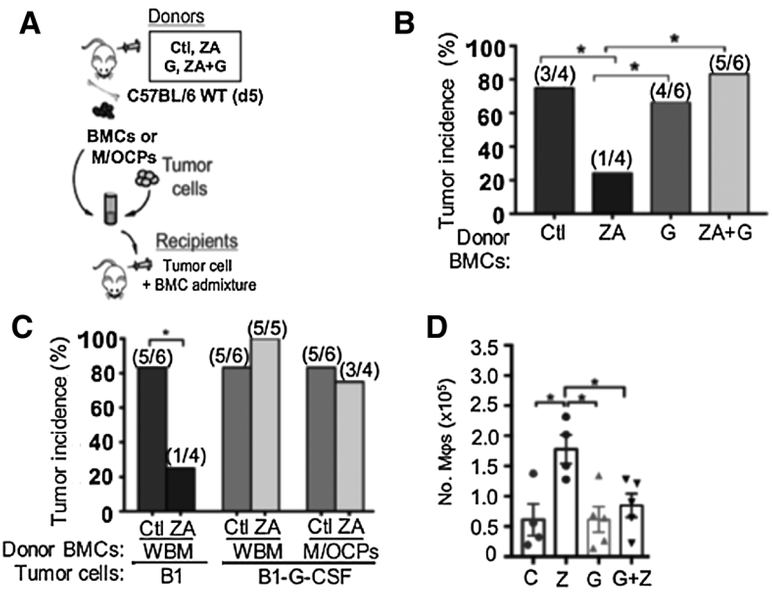

Figure 4.

G-CSF prevents generation of tumor-suppressive M/OCPs. **A,** Experimental scheme for assay to test tumor support function of BMCs from indicated donor mice. **B,** Incidence (%) of subcutaneous tumor formation in nude recipient mice at experimental endpoint (d14) resulting from B1 cells admixed with WBM from Ctl-, ZA-, G-CSF (G)-, or ZA+G-CSF (ZA+G)-treated C57BL/6 donors ($n = 4$–6 tumors per cohort; statistics representative of two biological replicates). **C,** Incidence (%) of tumor formation in nude recipient mice at experimental endpoint (d14) resulting from B1 or B1-G cells admixed with WBM or sorted M/OCPs from Ctl- or ZA-treated C57BL/6 donors ($n = 4$–6 tumors per cohort; statistics representative of two biological replicates). **D,** Quantitative flow cytometric analysis of WBM from indicated mice for number of macrophages ($Cd11b^+/F4/80^+/MHCII^+$) 3 days after Ctl (C), ZA (Z), G-CSF (G), or G-CSF+ZA (G+Z) treatment ($n = 4$-5/cohort; representative of three biological replications). Error bars, mean ± SEM; two-tailed *t*- ests (unpaired) were used to determine statistical significance (*, $P < 0.05$).

high G-CSF expression, to generate G-CSF–low cell lines (B2-shG1 and B2-shG2; Supplementary Fig. S3E). At this time point, metastatic burden was not significantly affected following ZA pretreatment regardless of G-CSF status in the B2 cells (Fig. 3B and C; Supplementary Fig. S3J). Likewise, neutralizing G-CSF *in vivo* prior to IC injection of the B2 cell line did not significantly reduce metastases following ZA pretreatment (Fig. 3D).

Together, these findings demonstrated that elevating G-CSF levels is sufficient to confer ZA resistance, but that suppression of G-CSF is not sufficient to induce ZA response. Moreover, these data indicated that G-CSF alone does not necessarily enhance metastatic burden above that of controls, but suggested that in the context of ZA treatment, G-CSF increases metastatic burden.

G-CSF prevents generation of tumor-suppressive M/OCPs

We next wondered whether resistance to ZA under G-CSF–high conditions was due to counteracting effects of G-CSF on bone marrow hematopoietic cells. We started by analyzing the function of WBM harvested from C57BL/6 mice 5 days following administration of ZA, G-CSF, combination ZA+G-CSF, or vehicle control (Fig. 4A).

As we observed repeatedly, WBM from ZA-treated mice inhibited B1 tumor formation *in vivo* (Fig. 4B; Supplementary Fig. S4A). We also confirmed that, as expected, ZA decreased osteoclast activity in these mice (Supplementary Fig. S4B). While WBM from mice treated systemically with G-CSF did not significantly alter tumor growth relative to that of the control cohort, when mice were treated systemically with combination ZA+G-CSF, their WBM was no longer tumor suppressive (Fig. 4B; Supplementary Fig. S4A). Importantly, both WBM and M/OCPs harvested from ZA-treated mice, which inhibited outgrowth of B1 tumor cells, were unable to inhibit growth of B1 tumor cells that overexpressed G-CSF (B1-G; Fig. 4C; Supplementary Fig. S4C).

In concordance with our findings from the *in vitro* differentiation assays (Fig. 2C and D), ZA significantly increased the numbers of macrophages in the marrow relative to vehicle control *in vivo* (Fig. 4D). In contrast, WBM from mice treated systemically with G-CSF or with ZA+G-CSF contained similar numbers of macrophages as those of the Ctl cohort (Fig. 4D).

These results suggested that G-CSF itself does not generate a marrow environment that enhances tumor growth relative to the control cohorts. Instead, G-CSF appeared to render ZA ineffective to generate tumor-suppressive marrow.

G-CSF counteracts ZA's ability to push differentiation of myeloid/osteoclast progenitors toward phagocytic macrophages

Our results thus far established that ZA alters the lineage potential of M/OCPs and renders them tumor-suppressive, while G-CSF mediates resistance to their tumor-suppressive effect. We therefore wished to know whether G-CSF alters the lineage potential of the M/OCP population.

We first isolated WBM from Ctl-, ZA-, G-CSF, and ZA+G-CSF–treated mice and then treated the cells *in vitro* with M-CSF and RANKL (Fig. 5A). As we repeatedly observed, in the absence of G-CSF, WBM from the ZA-treated cohort gave rise to significantly fewer osteoclasts than those from the control cohorts (Fig. 5B). However, WBM from G-CSF–treated animals gave rise to significantly more osteoclasts, even in the context of ZA treatment (Fig. 5B).

We also isolated M/OCPs from Ctl- or ZA-treated mice and then treated the cells *in vitro* with M-CSF and RANKL in the presence or absence of G-CSF (Fig. 5C). In the presence of G-CSF, M/OCPs from both Ctl- and ZA-treated mice gave rise to increased numbers of osteoclasts and decreased numbers of macrophages *in vitro* relative to M/OCPs in the absence of G-CSF (Fig. 5D and E; Supplementary Fig. S5A and S5B).

Our RNAseq analyses of M/OCPs from Ctl and ZA-treated mice (Fig. 1F) had suggested that ZA induces transcriptional changes consistent with monocyte/macrophage lineage bias. Therefore, to test potential functional consequences of altered M/OCP lineage potential, we added fluorescently labeled B1 tumor cells to the cultures resulting from M/OCP differentiation under various conditions, thus enabling us to assess

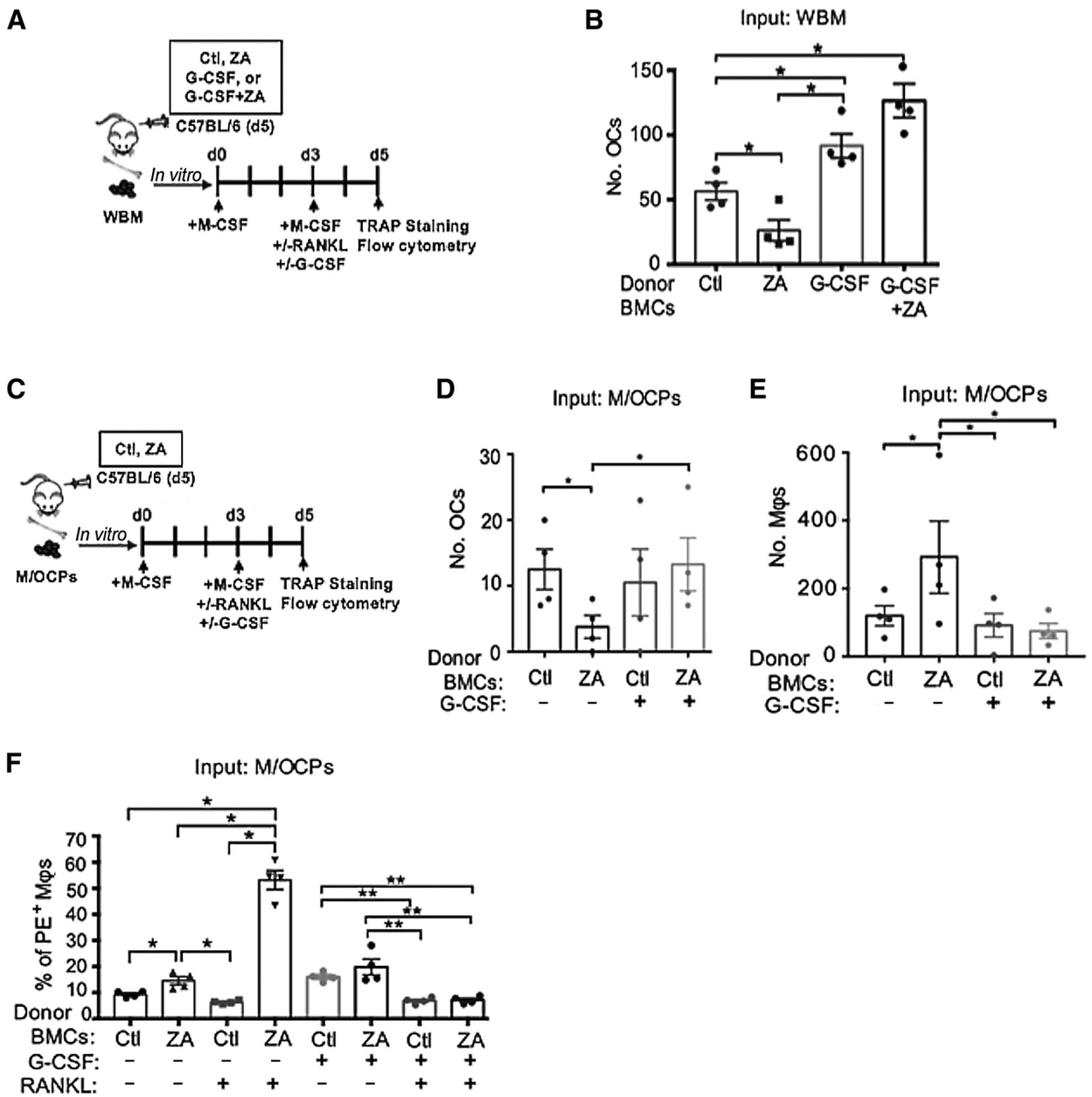

Figure 5.

G-CSF counteracts ZA's ability to push differentiation of myeloid/osteoclast progenitors toward phagocytic macrophages. **A,** Experimental scheme for *in vitro* osteoclast differentiation assay using bone marrow from Ctl-, ZA-, G-CSF- or ZA+G-CSF-treated C57BL/6 donors. **B,** Quantification of osteoclasts (OC; $TRAP^+$, multinucleated cells) at endpoint (d5) of *in vitro* osteoclast differentiation assay with 1,000 WBM per well from Ctl-, ZA-, G-CSF-, or ZA+G-CSF–treated C57BL/6 donors ($n = 4$ donor samples/cohort; representative of three biological replicates). **C,** Experimental scheme for *in vitro* osteoclast differentiation assay using bone marrow from Ctl- or ZA-treated C57BL/6 donors that were subsequently treated with Ctl or recombinant hG-CSF *in vitro* at d3. **D,** Quantification of osteoclasts ($TRAP^+$, multinucleated cells) at endpoint (d5) of *in vitro* osteoclast differentiation assay with 250 M/OCPs per well from Ctl- or ZA-treated C57BL/6 donor mice; M/OCPs were treated *in vitro* with RANKL ± G-CSF ($n = 4$ donor samples per cohort; representative of three biological replications). **E,** Flow cytometric quantification of macrophages ($Cd11b^+$/F4/80 $MHCII^+$) at endpoint of *in vitro* osteoclast differentiation assay (d5) using sorted M/OCPs from Ctl- or ZA-treated C57BL/6 mice; M/OCPs were subsequently treated *in vitro* with M-CSF and RANKL ± G-CSF ($n = 4$ donor samples per cohort; representative of three biological replicates). **F,** Percent of phycoerythrin (PE)-positive M/OCP-derived macrophages ($Cd11b^+$ F4/80^+ $MHCII^+$) at endpoint (d5), indicating phagocytosis of Did-Cm (PE)-labeled B1 tumor cells ($n = 4$ donor samples per cohort; representative of three biological replicates). Error bars, mean ± SEM; two-tailed *t* tests (unpaired) were used to determine statistical significance (*, $P < 0.05$; **, $P < 0.01$).

macrophage phagocytic capacity by scoring their uptake of fluorescence. In the absence of G-CSF, macrophages derived from M/OCPs of ZA-treated mice had significantly enhanced phagocytic capacity relative to those from Ctl-treated mice, irrespective of adding RANKL to the culture (Fig. 5F). In contrast, G-CSF significantly decreased the phagocytic capacity of the resulting culture from ZA-treated M/OCPs in both the undifferentiated (without RANKL) and differentiated (with RANKL) cultures (Fig. 5F). Consistent with the phagocytic phenotype, numbers of F4/80 MHCII+ macrophages in the bone marrow of ZA-treated mice was approximately 3-fold higher than in the control cohort, and G-CSF prevented this increase (Supplementary Fig. S5C).

Collectively, these findings suggested that G-CSF counteracts the effect of ZA on M/OCP function and lineage potential at least in part by preventing ZA from inducing M/OCP differentiation toward phagocytic macrophages. Moreover, these results provide additional evidence to suggest an association between lineage potential and the tumor-inhibitory function of the bone marrow.

Bone marrow transcriptome and gene ontology processes that correlate with function

The results from our preclinical metastasis models thus far indicated that the status of the bone marrow at the time metastatic tumor cells encounter it has a profound influence on metastatic success. As such, we wanted to gain insights into how the whole bone marrow hematopoietic microenvironment is affected by ZA and how G-CSF may alter the ZA signature. We therefore characterized transcriptional programs (RNA-seq) on whole bone marrow from mice treated with Ctl, ZA, G-CSF, or combination ZA+G-CSF (GSE108250).

We first analyzed the RNA-seq data by identifying enriched gene ontology processes (36) within the lists of DEGs from each treatment condition (ZA, G-CSF, or ZA+G-CSF) as compared with Ctl-treated bone marrow (Supplementary Fig. S6A–S6C; Supplementary Table S3A–S3F). In the ZA-treated cohort, significantly enriched processes were related primarily to metabolic process whereas in the G-CSF–treated cohorts, as well as in the ZA+G-CSF–treated cohorts, significantly enriched processes were dominated by immune processes (Supplementary Fig. S6C).

A global analysis of gene expression differences between each of the 3 treatment cohorts (ZA, G-CSF, and ZA+G-CSF) and the control cohort (Ctl) provided insights into the effect of each treatment on WBM and M/OCPs. For WBM, the comparisons identified 56, 1,445, and 1,054 DEGs (modified BH adjusted P value <0.01) in the ZA, G-CSF, and ZA+G-CSF cohorts, respectively (Fig. 6A; Supplementary Fig. S6A and S6B; Supplementary Table S4A–S4C). A total of 779 DEGs were common to both the G-CSF and ZA+G-CSF comparisons, only 28 of which were also shared with the ZA comparison (Fig. 6A). The 28 DEGs that were affected by all 3 treatments were the only DEGs shared between the ZA and ZA+G-CSF comparisons (Fig. 6A). Importantly, 16 DEGs were affected exclusively by ZA treatment (i.e., not identified in the combined treatment comparison) and included genes involved in phagocytosis such as *Slc15a4*, *Usp37*, and *Ipo13* (Fig. 6A; Supplementary Table S4A). Interestingly, approximately 25% of the DEGs resulting from combination ZA+G-CSF were unique to that treatment cohort (Fig. 6A).

In the M/OCPs, 165 DEGs resulted from ZA treatment, 314 from G-CSF treatment, and 151 from combination ZA+G-CSF (Fig. 6A; Supplementary Table S5A–S5C). As observed with WBM, a number of DEGs (~38%) were unique to the combination treatment. 103 DEGs were affected exclusively by ZA treatment (Fig. 6A). Interestingly, *Mapk8ip2* was one of the most significantly upregulated DEGs in the ZA-treated cohort ($P = 3.39 \times 10^{-14}$), but was down-regulated in both G-CSF–treated ($P < 8.48 \times 10^{-4}$), and ZA+G-CSF–treated cohorts ($P = 4.31 \times 10^{-6}$). *Mapk8ip2* is involved in monocyte differentiation into macrophages when activated (Supplementary Table S5A; ref. 37).

These analyses revealed that both G-CSF and ZA significantly and uniquely affect transcriptional programs in the WBM and that combined treatment yields yet a different transcriptional profile from either treatment alone. Moreover, ZA treatment appeared to have a larger impact on M/OCPs than on WBM, while G-CSF appeared to dominate the effect on WBM.

Effects of ZA that are lost or significantly changed in the presence of G-CSF

We considered the transcriptional effects we observed with each treatment and the fact that ZA treatment generated metastasis-suppressive marrow while G-CSF alone had no effect on metastatic burden, yet G-CSF induced resistance to ZA and increased metastatic burden in the context of ZA treatment. In doing so, we speculated that ZA and G-CSF either affect the marrow in opposing directions or that the effects of combination treatment cannot be explained by contributions of either treatment alone.

Our comparative analysis revealed that the DEGs upon combination treatment were not equivalently significant in either the ZA or G-CSF cohorts (Fig. 6A). In other words, none of these genes was expressed in an opposing manner. Indeed, 263 DEGs were unique to WBM and 58 genes unique to the M/OCP population in the ZA+G-CSF cohorts (Fig. 6A). Hence, we employed a regression approach with an interaction term and identified genes for which the effects of G-CSF and ZA statistically interact (Fig. 6B; Supplementary Table S6A and S6B).

GO analysis of these nonadditively differentially expressed genes from WBM revealed processes significantly enriched by the combination treatment that described the difference in response to ZA in the presence of G-CSF (Fig. 6C; Supplementary Table S7). The enrichment list represents gene sets that were either enhanced or ablated relative to the cumulative effects expected from adding together the effects of ZA and G-CSF treatments alone, including those newly emerging with combination treatment. Of these, "immune response" and "phagocytosis" were particularly intriguing to us, as these were predominantly suppressed by combination treatment. For example, a number of genes involved in antigen processing and lymphocyte activation, including *B2m*, *Vav2*, and a number of histocompatibility genes (*H2-K1*, *H2-D1*, *H2-Q5*, *H2-Q7*) were uniquely suppressed with ZA+G-CSF combination treatment relative to Ctl treatment (Supplementary Table S6A). Moreover, *Axl*, which suppresses myeloid cell immune function and dampens NK-cell activity (38), was significantly suppressed by ZA treatment [$\log_2$ (fold change) $= -1.20$, $P = 1.25 \times 10^{-4}$] but significantly enhanced with ZA+G-CSF treatment [$\log_2$ (fold change) $= 1.68$, $P = 2.7 \times 10^{-5}$; Supplementary Table S6A].

Together with our preclinical modeling, these analyses indicated that in the marrow of animals treated with combination

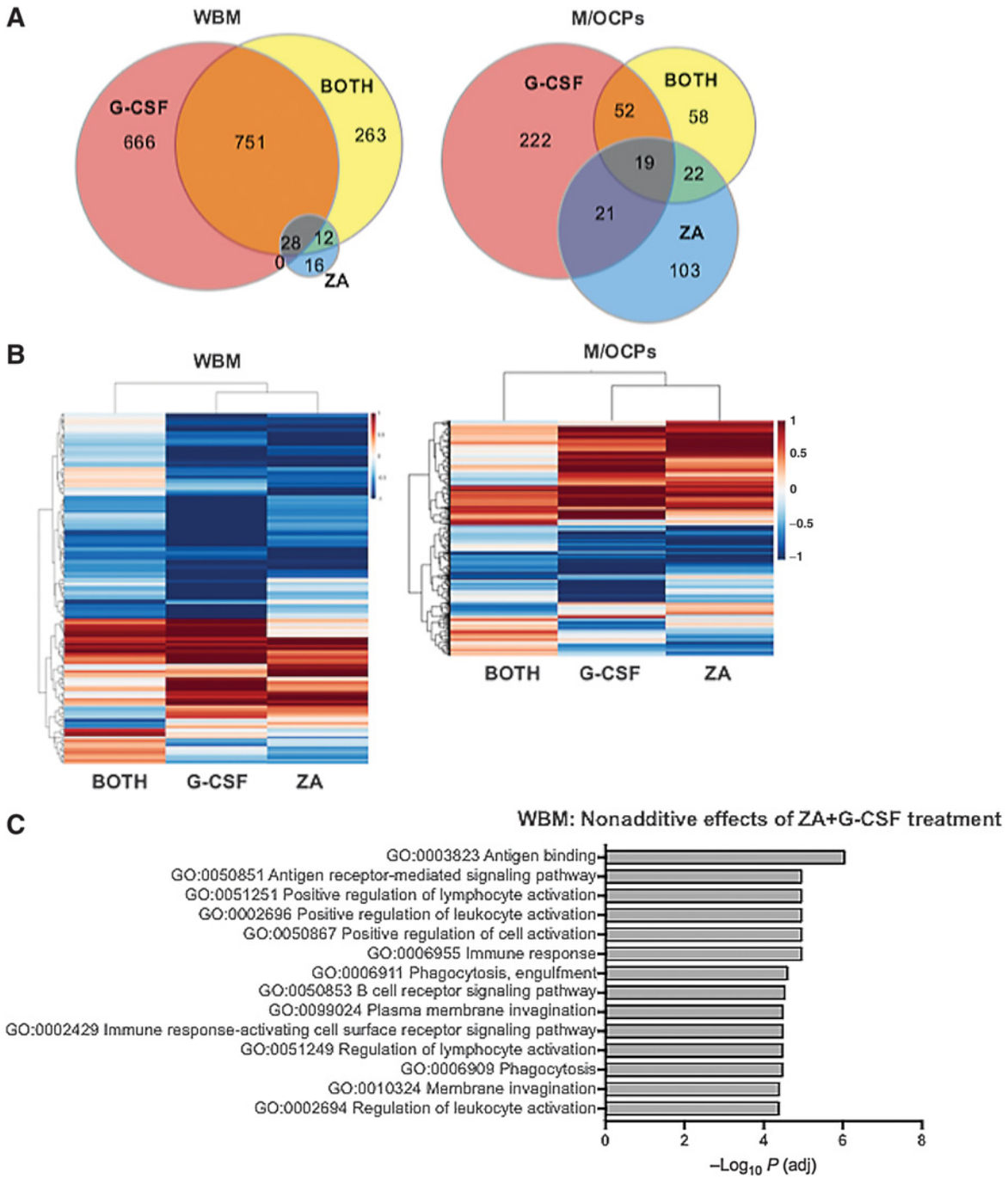

Figure 6.

Bone marrow transcriptome and gene ontology processes that correlate with function. **A,** Venn diagrams for distinct and nondistinct differentially expressed genes in the bone marrow (left) or M/OCPs (right) from mice treated with ZA (blue), G-CSF (red), or ZA+G-CSF ("Both"; yellow), as normalized to Ctl-treated bone marrow or M/OCPs (modified BH adjusted *P* value less than 0.01). **B,** Heatmap of expression levels of genes identified from a regression analysis of the interaction between G-CSF and ZA effects on gene expression for WBM (left) or M/OCPs (right). Individual sample expression levels are shown for genes with a modified BH-adjusted *P* value of less than 0.01 from the regression. Values represent normalized counts after centering on the mean expression levels of the control samples and scaling to the range of gene expression across all samples (so that −1 represents the lowest expression level for all samples and 1 the highest). **C,** Enriched gene ontology categories for genes for which the simultaneous effects of G-CSF and ZA treatment on expression were not additive in a comparative analysis model for WBM. Categories for each indicated cohort were compared with control using the nonadditive genes (as ordered by absolute $\log_2$-fold change; modified BH-adjusted *P* value less than 0.01). A list of the statistically enriched GO terms for biological processes was generated using the methods described in **A**.

ZA + G-CSF, the transcriptional effects of ZA are negated and/or significantly changed by G-CSF in a manner that associates with metastatic progression.

High plasma G-CSF correlates with worse outcome for patients with breast cancer treated with adjuvant ZA

Our preclinical data established that G-CSF mediates resistance to ZA, and in fact, ZA+G-CSF combination treatment had unexpected effects on the metastatic microenvironment, resulting in enhanced metastasis relative to ZA treatment alone. Hence, we sought to understand whether patient plasma G-CSF levels correlate with response to ZA. In the clinical setting, bisphosphonates have suggested benefit, as demonstrated by results from a meta-analysis in which patients who had received adjuvant bisphosphonate treatment observed a significant reduction in breast cancer recurrence in the bone (39). Nevertheless, responses have been limited for unknown reasons and biomarkers that can be used to guide treatment decisions are lacking.

We analyzed patient plasma samples (n = 392) from the AZURE clinical trial in which women with stage II/III breast cancer were randomized to receive standard systemic treatment (>95% of the patients received chemotherapy) with or without adjuvant ZA (Fig. 7A; ref. 16). In the AZURE trial, postmenopausal (natural or induced with ovarian suppression) patients observed a significant decrease in overall breast cancer recurrence (16). Importantly, primary G-CSF prophylaxis was not used in these patients. We verified that the magnitude of effect of ZA in reducing the development of bone metastasis at any time during the 10-year follow-up in our patient subset was similar to that of the overall trial [trial total n = 3,360, HR = 0.81, 95% confidence interval (CI) 0.68–0.97 (16); our subset n = 392, HR = 0.89, 95% CI 0.62–1.3; Fig. 7A].

We utilized an analytic approach that adjusts for an optimal plasma G-CSF concentration cut-off point and enables us to accurately determine DFS and significance levels in an unbiased fashion (See Materials and Methods, Supplementary Fig. S7A–S7D; ref. 40). On the basis of these previously published methods, we determined that a plasma G-CSF concentration of 23 pg/mL was the optimum cut-off point for assessing disease-free survival (DFS) events in ZA-treated patients (40).

Patients receiving adjuvant ZA whose plasma G-CSF levels were > 23 pg/mL at the time of randomization had significantly reduced DFS when compared with patients with plasma G-CSF levels < 23 pg/mL ($P_{adjusted}$ = 0.02) as assessed over a 10-year period (Fig. 7B). However, in the cohort that did not receive ZA, plasma G-CSF levels did not predict a significant difference in DFS (Supplementary Fig. S7B). Cox model analysis

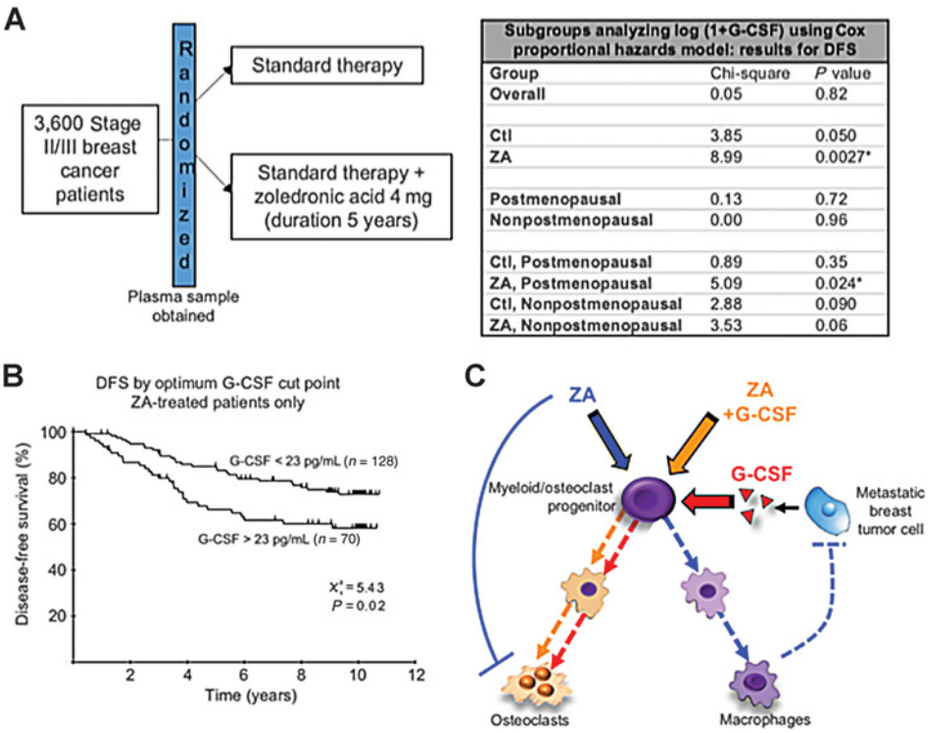

Subgroups analyzing log (1+G-CSF) using Cox proportional hazards model: results for DFS		
Group	Chi-square	P value
Overall	0.05	0.82
Ctl	3.85	0.050
ZA	8.99	0.0027*
Postmenopausal	0.13	0.72
Nonpostmenopausal	0.00	0.96
Ctl, Postmenopausal	0.89	0.35
ZA, Postmenopausal	5.09	0.024*
Ctl, Nonpostmenopausal	2.88	0.090
ZA, Nonpostmenopausal	3.53	0.06

Figure 7.

High plasma G-CSF correlates with worse outcome for patients with breast cancer treated with adjuvant ZA. **A,** AZURE clinical trial randomization scheme from Coleman and colleagues, 2014 (16) and Cox proportional hazards model analysis of subgroup from AZURE trial (n = 392) for DFS by Ctl and ZA cohorts, menopausal status, and by menopausal status for treatment group (*, P < 0.05). **B,** DFS outcome (derived from cut-off point analysis—see Materials and Methods) defined in terms of number of DFS events avoided/saved over the 10-year period post randomization among ZA-treated patients; optimal cut-off point was at 23 pg/mL G-CSF. **C,** Proposed model. ZA inhibits mature osteoclasts and also increases the numbers of M/OCPs in the bone marrow, altering their gene expression profile to drive them toward tumor suppressive phagocytic macrophages. Tumor-derived or systemic G-CSF counteracts the effects of ZA by driving the lineage potential of M/OCPs toward osteoclasts.

demonstrated that the relationship between high plasma G-CSF levels and DFS in ZA-treated patients could not be explained by imbalances in other key prognostic variables, namely number of involved lymph nodes affected, tumor size (T stage), and breast cancer receptor status (ER/PR/Her2). Moreover, in support of the retrospective analyses demonstrating that postmenopausal patients observed significant benefit with adjuvant ZA, plasma G-CSF levels were significantly lower in postmenopausal patients than premenopausal patients in our cohort ($P = 1.14 \times 10^{-4}$).

Discussion

This work revealed that bone marrow hematopoietic cell states, particularly M/OCP lineage potential, have a profound impact on breast cancer bone metastasis and that the hematopoietic microenvironment, which serves as a niche for disseminated tumor cells, can be modulated by bone-targeting agents and cytokines to alter disease outcome. Specifically, the bisphosphonate, ZA, directs M/OCP lineage potential toward tumor-suppressive macrophages and prevents metastatic growth in the bone; systemic or tumor-derived G-CSF promotes resistance to the metastasis-suppressive effect of ZA by skewing M/OCP differentiation toward osteoclasts and away from the phagocytic myeloid lineage (Fig. 7C).

Further mechanistic investigation into the newly identified biology that we report here is warranted to understand how best to capitalize on bone marrow and M/OCP function and differentiation potential to prevent or limit metastatic disease in the bone. The novel, perhaps unexpected effect of ZA on the bone microenvironment may provide one such avenue. From a clinical perspective, targeting osteoclast activity with bone-modifying agents, such as bisphosphonates or the RANK-ligand inhibitor denosumab, has significantly reduced skeletal-related events patients with metastatic breast cancer to the bone (i.e., bone fractures, bone pain requiring radiotherapy, spinal cord compression, and hypercalcemia; ref. 41). Thus, current NCCN guidelines support the administration of these agents in combination with chemotherapy or endocrine therapy for patients with bone metastases (category 1 recommendation; refs. 42, 43). Results from a meta-analysis of individual patient data from 18,766 women—enrolled over 26 randomized trials that evaluated the benefits of adjuvant bisphosphonate treatment—showed a significant reduction in bone recurrence and improvement in breast cancer–specific survival (44).

Subgroup analyses have suggested that postmenopausal status, but not hormone receptor (ER/PR) or growth factor receptor (Her2) expression, predisposes patients who are more likely to benefit from bisphosphonates, and this is reflected in the recently published guidelines by Cancer Care Ontario and the American Society of Clinical Oncology that recommend consideration of ZA or clodronate for postmenopausal (natural or induced with ovarian suppression) patients deemed candidates for adjuvant systemic therapy (43). Other meta-analyses revealed that adjuvant therapy with ZA increases overall survival in early-stage breast cancer (44). In addition, ZA decreased the number of DTCs in the bone marrow of stage II/III patients with breast cancer in a randomized clinical trial (45). ZA has also been demonstrated to increase disease-free survival when it is administered with neoadjuvant chemotherapy, particularly in postmenopausal patients (46). Nevertheless, an underlying biological explanation for the protective effect of bisphosphonates in breast cancer, in terms of reduction of disease recurrence, had remained elusive.

Although meta-analyses of the clinical studies highlighted efficacy of ZA, no overall survival benefit has been reported to date in individual randomized controlled trials in breast cancer. Consequently, even considering pre- or post-menopausal status, it remained unclear how to identify which patients would observe benefit with ZA (16). Our findings provide new insights into why certain patients may not see reduction in breast cancer recurrence with ZA. Our preclinical findings are underscored by the fact that patients in the AZURE trial (16) with higher plasma G-CSF levels experienced worse outcome from adjuvant ZA treatment and provide preliminary evidence to caution against the use of ZA in patients with high plasma G-CSF. High plasma G-CSF, however, has been correlated with poor prognosis in patients with breast cancer, specifically those with triple-negative breast cancer (32). However, in our study, plasma G-CSF levels alone, in the absence of ZA treatment, did not predict worse survival.

Unfortunately, our findings provide a preliminary indication that suppression of G-CSF may not be an effective strategy for improving responses to ZA, as neither genetic nor pharmacologic inhibition of G-CSF was sufficient to confer response. It is possible that the balance between tumor-promoting (8) and tumor-suppressive cells in the marrow, or other cytokines (such as GM-CSF) must be considered in the appropriate contexts. Further studies to evaluate our findings will therefore require well-designed preclinical and clinical trials to determine patient benefit with adjuvant ZA in the presence or absence of G-CSF administration. Our analyses suggest other ways to achieve this goal may be to include combinations with other bone-targeting agents or immunotherapies. Further studies based on results of our gene expression profiling under these various conditions may reveal factors, pathways, and processes that are necessary and/or sufficient for the tumor-inhibitory function of the bone marrow. Some of the newly identified gene products presented here may be considered as candidate targets for future combination therapies and preclinical research.

Likewise, additional work will be necessary to determine the translatability of G-CSF as a biomarker for selection of patients who should/should not receive ZA treatment, given that many patients also receive G-CSF at the time of chemotherapy and adjuvant ZA treatment (the patients in our study did not receive primary G-CSF prophylaxis and less than 10% received secondary G-CSF treatment). Identifying biomarkers that better stratify patient risk and responses to ZA hold the potential of using bone-modulating drugs to improve patient outcomes.

Identification of a tumor-suppressive population in the bone marrow provides opportunities for exploring new therapeutic strategies that could generate such cells to halt metastatic progression or overcome the adverse effects of G-CSF. The ability to use relatively safe bone-modulating therapeutics to capitalize on the tumor-suppressive function of the bone marrow, particularly M/OCP populations, provides a foundation for potentially curative treatments during the time when metastatic breast cancer can still be controlled.

Disclosure of Potential Conflicts of Interest

J.E. Brown has received speakers bureau honoraria from Amgen and Novartis and is a consultant/advisory board member for Amgen and Novartis. R.E. Coleman is a medical director at prIME Oncology, has ownership interest (including stock, patents, etc.) in Inbiomotion, and is a consultant/advisory board member for Amgen. No potential conflicts of interest were disclosed by the other authors.

Authors' Contributions

Conception and design: J.M. Ubellacker, J.E. Brown, Y. Qin, S.S. McAllister
Development of methodology: J.M. Ubellacker, J.E. Brown, S.S. McAllister
Acquisition of data (provided animals, acquired and managed patients, provided facilities, etc.): J.M. Ubellacker, N. Baryawno, N. Severe, M.J. DeCristo, M.-T. Haider, C.S. Rhee, Y. Qin, I. Holen, R.E. Coleman
Analysis and interpretation of data (e.g., statistical analysis, biostatistics, computational analysis): J.M. Ubellacker, N. Severe, J. Sceneay, J.N. Hutchinson, M.-T. Haider, C.S. Rhee, W.M. Gregory, A.C. Garrido-Castro, J.E. Brown, D.T. Scadden, S.S. McAllister
Writing, review, and/or revision of the manuscript: J.M. Ubellacker, N. Baryawno, N. Severe, J.N. Hutchinson, W.M. Gregory, A.C. Garrido-Castro, I. Holen, J.E. Brown, R.E. Coleman, D.T. Scadden, S.S. McAllister
Administrative, technical, or material support (i.e., reporting or organizing data, constructing databases): J.N. Hutchinson
Study supervision: S.S. McAllister

Acknowledgments

This work was supported by funds from NIH T32 GM007226 and NCI F31CA195797 (to J. Ubellacker); NIH R01DK107784 and U54CA163191 (to D. Scadden); DOD Era of Hope W81XWH-14-1-0191 and NIH NCI RO1 CA166284 Presidential Early Career Award for Scientists and Engineers (to S. McAllister). We are grateful to the patients who participated in the AZURE trial. We thank P. Ottewell and G. van der Plujm for generous donation of MDA-MB-231 bone-tropic cell lines; J. Brown, H. Shulver, and J. Horsman for assistance with obtaining clinical trial samples; and the Boston Children's Hospital Heme/Onc-HSCI Flow Cytometry facility (Boston, MA). We thank members of the McAllister and Scadden laboratories and Drs. Bruce Zetter, Karen Cichowski and Nancy Lin for helpful discussion; L. Rooney, J. Olive, Z. Castano for technical review of the manuscript; J. Ferlic for biostatistics assistance; R. Tadipatri for technical assistance; A. Molineaux and M. Petit for administrative assistance. We are also grateful to N. Tung and J. Garber for helpful discussion in early stages of the project.

The costs of publication of this article were defrayed in part by the payment of page charges. This article must therefore be hereby marked *advertisement* in accordance with 18 U.S.C. Section 1734 solely to indicate this fact.

Received February 20, 2018; revised June 12, 2018; accepted July 23, 2018; published first July 31, 2018.

References

1. Colleoni M, Sun Z, Price KN, Karlsson P, Forbes JF, Thurlimann B, et al. Annual hazard rates of recurrence for breast cancer during 24 years of follow-up: results from the International breast cancer study group trials I to V. J Clin Oncol 2016;34:927–935.
2. Press DJ, Miller ME, Liederbach E, et al. De novo metastasis in breast cancer: occurrence and overall survival stratified by molecular subtype. Clin Ex Metastasis 2017;1573–7276.
3. Gnant M, Hadji P. Prevention of bone metastases and management of bone health in early breast cancer. Breast Cancer Res 2010;12: 216.
4. Tjensvoll K, Oltedal S, Heikkila R. Persistent tumor cells in bone marrow of non-metastatic breast cancer patients after primary surgery are associated with inferior outcome. BMC Cancer 2012;12:190. doi: 10.1186/1471-2407-12-190.
5. Ren G, Esposito M, Kang Y. Bone metastasis and the metastatic niche. J Mol Med 2015;93:1203–12.
6. Guise T. Examining the metastatic niche: targeting the microenvironment. Semin Oncol 2010;37:S2–S14.
7. Rack B, Junckstock J, Gunthner-Biller M, Andergassen U, Neugebauer J, Hepp P, et al. Trastuzumab Clears HER2/neu-positive isolated tumor cells from bone marrow in primary breast cancer patients. Arch Gynecol Obstet 2011;285:485–92.
8. McAllister SS, Weinberg RA. The tumour-induced systemic environment as a critical regulator of cancer progression and metastasis. Nat Cell Biol 2014;16:717–27.
9. Engblom C, Pfirschke C, Pittet MJ. The role of myeloid cells in cancer therapies. Nature Rev Cancer 2016;16:447–62.
10. Gao D, Mittal V. The role of bone-marrow-derived cells in tumor growth, metastasis initiation and progression. Trends Mol Med 2009;15:333–43.
11. Morrison SJ, Scadden DT. The bone marrow niche for haematopoietic stem cells. Nature 2014;505:327–34.
12. Kollet O, Dar A, Shivtiel S, Kalinkovich A, Lapid K, Sztainberg Y, et al. Osteoclasts degrade endosteal components and promote mobilization of hematopoietic progenitor cells. Nat Med 2006;12:657–64.
13. Nilsson SK, Johnston HM, Whitty GA, Williams B, Webb RJ, Denhardt DT, et al. Osteopontin, a key component of the hematopoietic stem cell niche and regulator of primitive hematopoietic progenitor cells. Blood 2005;106:1232–9.
14. Stier S, Ko Y, Forkert R, Lutz C, Neuhaus T, Grunewald E, et al. Osteopontin is a hematopoietic stem cell niche component that negatively regulates stem cell pool size. J Exp Med 2005;201:1781–91.
15. Ubellacker JM, Haider MT, DeCristo MJ, Allocca G, Brown NJ, Silver DP, et al. Zoledronic acid alters hematopoiesis and generates breast tumor-suppressive bone marrow cells. Breast Cancer Res 2017;19:23.
16. Coleman R, Cameron D, Dodwell D, Bell R, Wilson C, Rathbone E, et al. Adjuvant zoledronic acid in patients with early breast cancer: final efficacy analysis of the AZURE (BIG 01/04) randomised open-label phase 3 trial. Lancet Oncol 2014;15:997–1006.
17. Marsh T, Wong I, Sceneay J, Barakat A, Qin Y, Sjodin A, et al. Hematopoietic age at onset of triple-negative breast cancer dictates disease aggressiveness and progression. Cancer Res 2016;76:2932–43.
18. McAllister SS, Gifford AM, Greiner AL, Kelleher SP, Saelzler MP, Ince TA, et al. Systemic endocrine instigation of indolent tumor growth requires osteopontin. Cell 2008;133:994–1005.
19. Boyle WJ, Simonet WS, Lacey DL. Osteoclast differentiation and activation. Nature 2003;423:337–42.
20. Jacome-Galarza CE, Lee SK, Lorenzo JA, Aguila JA. Identification, characterization and isolation of common progenitor for osteoclasts, macrophages, and dendritic cells from murine bone marrow and periphery. J Bone Miner Res 2013;28:203.
21. Miyamoto T. Identification and characterization of osteoclast precursor cells. BoneKEy 2013;346. doi: 10.1038/bonekey.2013.80.
22. Zhu L, Zhao Q, Yang T, Ding W, Zhao Y. Cellular metabolism and macrophage functional polarization. Int Rev Immunol 2015;34: 82–100.
23. Martinez F, Gordon S, Locati M, Mantovani A. Transcriptional profiling of the human monocyte-to-macrophage differentiation and polarization: new molecules and patterns of expression. J Immunol 2006;177: 7303–11.
24. Hirbe AC, Roelofs AJ, Floyd DH, Deng H, Becker SN, Lanigan LG, et al. The bisphosphonate zoledronic acid decreases tumor growth in bone in mice with defective osteoclasts. Bone 2009;44:908–16.
25. Zhang K, Kim S, Cremasco V, Hirbe AC, Novack DV, Weilbaecher K, et al. CD8+ T cells regulate bone tumor burden independent of osteoclast resorption. Cancer Res 2011;71:4799–808.
26. Dougall WC, Glaccum M, Charrier K, Rohrbach K, Brasel K, De Smedt T, et al. RANK is essential for osteoclast and lymph node development. Genes Dev 1999;13:2412–24.
27. Ari F, Miyamoto T, Ohneda O, Inada T, Sudo T, Brasel K, et al. Commitment and differentiation of osteoclast precursor cells by the sequential expression of c-fms and RANK receptors. J Exp Med 1999; 190:1741–1754.

28. Wetterwald A, van der Pluijm G, Que I, Sijmons B, Buijs J, Kaperien M, et al. Optical imaging of cancer metastasis to bone: a mouse model of minimal residual disease. Am J Pathol 2002;160:1143–53.
29. Nutter F, Holen I, Brown HK, Cross SS, Evans CA, Walker M, et al. Different molecular profiles are associated with breast cancer cell homing compared to colonisation of bone—evidence using a novel bone-seeking cell line. Endocr Relat Cancer 2014;21:327–41.
30. Ell B, Kang Y. Bone Metastasis. Cell 2012;151:690.
31. Weilbaecher KN, Guise TA, McCauley LK. Cancer to bone: a fatal attraction. Nat Rev Cancer 2011;11:411–25.
32. Hollmén M, Karaman S, Schwager S, Lisibach A, Christiansen AJ, Maksimow M, et al. G-CSF regulates macrophage phenotype and associates with poor overall survival in human triple-negative breast cancer. Oncoimmunology 2015;5:e1115177.
33. Takahashi T, Wada T, Mori M, Kokai Y, Ishii S. Overexpression of the granulocyte colony-stimulating factor gene leads to osteoporosis in mice. Lab Invest 1996;74:827–34.
34. Hirbe AC, Uluckan O, Morgan EA, Eagleton MC, Prior JL, Piwnica-Worms D, et al. Granulocyte colony-stimulating factor enhances bone tumor growth in mice in an osteoclast-dependent manner. Blood 2007;109: 3424–31.
35. Christopher MJ, Link DC. Granulocyte colony-stimulating factor induces osteoblasts apoptosis and inhibits osteoblast differentiation. J Bone and Miner Res 2008;23:1765–74.
36. Reimand J, Kull M, Peterson H, Hansen J, Vilo J. G:Profiler-a web-based toolset for functional profiling of gene lists from large-scale experiments. Nucleic Acids Res 2007;35:W193–W200.
37. Hale KK, Trollinger D, Rihanek M, Manthey CL. Differential expression and activation of p38 mitogen-activated protein kinase α, β, γ and δ in inflammatory cell lineage. J Immunology 1999;162: 4246–52.
38. Ludwig KF, Du W, Sorrelle NB, Wnuk-Lipinska K, Topalovski M, Toombs JE, et al. Small molecule inhibition of Axl targets tumor immune suppression and enhances chemotherapy in pancreatic cancer. Cancer Res 2018;78:246–55.
39. Early Breast Cancer Trialists' Collaborative Group (EBCTCG). Adjuvant bisphosphonate treatment in early breast cancer: meta-analyses of individual patient data from randomised trials. Lancet 2015;386: 1353–61.
40. Viprey VF, Gregory VM, Corrias MV, Tchirkov A, Swerts K, Vicha A, et al. Neuroblastoma mRNAs predict outcome in children with stage 4 Neuroblastoma: a European HR-NBL1/SIOPEN Study. J Clin Oncol 2014;32:1074–83.
41. Stopeck AT, Lipton A, Body JJ, Steger GG, Tonkin K, de Boer RH, et al. Denosumab compared with zoledronic acid for the treatment of bone metastases in patients with advanced breast cancer: a randomized, double-blind study. J Clin Oncol 2010;28:5132–9.
42. Gradishar WJ, Anderson BO, Balassanian R, Blair SL, Burstein HJ, Cyr A, et al. Breast cancer, version 1.2017. NNCN guidelines insights. J Natl Compr Canc Netw 2017;15:433–51.
43. Dhesy-Thind S, Fletcher GG, Blanchette PS, Clemons MJ, Dillmon MS, Frank ES, et al. Use of adjuvant bisphosphonates and other bone-modifying agents in breast cancer: a cancer care ontario and american society of clinical oncology clinical practice guideline. J Clin Oncol 2017;35:2062–80.
44. Valachis A, Polyzos NP, Coleman RE, Gnant M, Eidtmann H, Brufsky AM, et al. Adjuvant therapy with zoledronic acid in patients with breast cancer: a systemic review and meta-analysis. Oncologist 2013;18:353–61.
45. Aft RL, Naughton M, Trinkaus K, Watson M, Ylagan L, Chavez-MacGregor, et al. Effect of zoledronic acid on disseminated tumour cells in women with locally advanced breast cancer: an open label, randomized, phase 2 trial. Lancet Oncol 2010;11:421–28.
46. Kroep JR, Charehbili A, Coleman RE, Aft RL, Hasegawa Y, Winter MC, et al. Effects of neoadjuvant chemotherapy with or without zoledronic acid on pathological response: a meta-analysis of randomized trials. Eur J Cancer 2016;54:57–63.